

Synthesis, structural characterization and anion binding studies of palladium macrocycles with hydrogen-bonding ligands†‡

Pilar Diaz,^a Jorge A. Tovilla,^{a,b} Pablo Ballester,^{b,c} Jordi Benet-Buchholz^b and Ramón Vilar^{*a,b}

Received 12th March 2007, Accepted 25th May 2007

First published as an Advance Article on the web 29th June 2007

DOI: 10.1039/b703660d

The reactions between [Pd(P–P)(OTf)₂] (where P–P = dppp or dpfp) and two different bipyridyl ligands (L¹ = 1,3-bis(4-pyridylmethyl)urea and L² = 1,3-bis(pyridinylmethyl)benzenedicarboxamide) containing hydrogen-bonding units have been studied. The X-ray crystal structures of three of these assemblies have been solved showing them to be the [2 + 2] metallo-macrocycles [Pd(P–P)(Lⁿ)₂](OTf)₄ [P–P = dppp, n = 1, (1); P–P = dppp, n = 2, (2); P–P = dpfp, n = 1, (3)]. To confirm whether the dimeric assembly of one of these species (1) is retained in solution, several investigations have been carried out. ¹H NMR studies in DMSO and high resolution ESI mass spectrometry have shown that 1 is in equilibrium with a larger [3 + 3] metallo-macrocycle. The equilibrium between these two species can be modified by changing the temperature, concentration or solvent. Also, addition of certain anions (e.g. [H₂PO₄][−]) to the mixture shifts the equilibrium favoring the formation of the [2 + 2] metallo-macrocycle over the [3 + 3] (initially present in a larger proportion).

Introduction

The synthesis of metallo-macrocycles and metallo-cages has received considerable attention over the past few years.^{1–8} This type of assemblies are particularly attractive since the structural and functional properties of metal centers can be combined with the recognition abilities of organic ligands to yield species that can act as hosts for specific guests. The selective recognition of guests in the hollow cavities of the metallo-macrocycles and cages can in turn have important potential applications in catalysis⁹ and in the development of chemical sensors.^{10–15} One of the most successful approaches to prepare metallo-assemblies is by self-assembly where carefully designed building blocks are brought together by coordination to metal centers with well defined geometries. This approach has been successfully employed by Fujita,^{2,5,8} Stang,^{1,4} Raymond,^{16,17} Hump and Saalfrank^{18–20} amongst several other groups to prepare a wide range of metallo-assemblies.

Often, the assembly process can be improved (or modified) by the presence of a template. Templating agents usually make use of non-covalent interactions such as electrostatic forces, H-bonding, π–π interactions and hydrophobic effects to pre-arrange a group of building blocks in a suitable geometry to yield the targeted assembly.^{21–24} When a specific set of building blocks can be combined in different ways to yield different assemblies that can continuously interconvert, the idea of a dynamic combinatorial

library (DCL) arises.^{25–28} Due to the dynamic equilibria established in a DCL, the stabilization of any given compound by addition of an external species can lead to amplifying its formation. Hence, the addition of a template to the library can shift the equilibrium toward the formation of the compound that yields the thermodynamically more stable host–template assembly. This approach—pioneered by Sanders²⁷ and Lehn²⁶—has already been used to successfully synthesise selective chemical receptors that are amplified from a DCL.

Although several reports have demonstrated that anions can be successfully employed as templates for the formation of a wide range of organic and metal–organic assemblies,^{29,30} to date there are only a handful of examples where anions are used as templates in DCLs.^{31–33}

Herein we report the synthesis of a series of metallo-macrocycles built from square planar [Pd(dppp)]²⁺ units and bis-pyridyl ligands containing hydrogen bonding units (see Fig. 1).

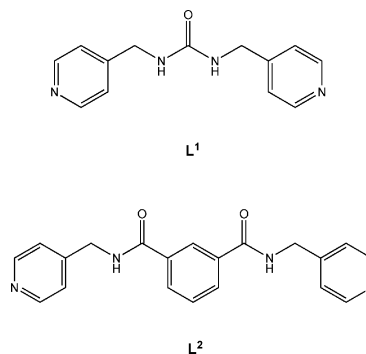


Fig. 1 Schematic representation of ligands L¹ and L².

Although a vast number of examples of metallo-macrocycles based on palladium(II) and platinum(II) centres and bis-pyridyls have been previously reported,^{10–13,34–46} in most cases the bis-pyridyl bridge is rigid and does not contain further functionalities.

^aDepartment of Chemistry, Imperial College London, London, UK SW7 2AZ. E-mail: r.vilar@imperial.ac.uk

^bThe Institute of Chemical Research of Catalonia, Avda. Països Catalans 16, 43007, Tarragona, Spain

^cInstitució Catalana de Recerca i Estudis Avançats (ICREA), Pg. Lluís Companys 23, 08010, Barcelona, Spain

† CCDC reference numbers 624779–62478 and 624783–624784. For crystallographic data in CIF or other electronic format see DOI: 10.1039/b703660d

‡ Electronic supplementary information (ESI) available: High resolution ESI mass spectrum of 1 (Fig. S1–S3). See DOI: 10.1039/b703660d

We rationalized that an increased geometrical flexibility on the bridging ligand—provided by CH₂ groups between the pyridines and the central spacer (see Fig. 1)—would potentially yield a wider range of metallo-macrocycles. Furthermore, only a few examples have been reported of metallo-macrocycles based on bis-pyridyl bridges containing hydrogen bonding groups.^{47–50} Since we have particular interest in the use of anions as templates to generate selective receptors for such species,^{51–57} hydrogen bonding units were introduced into ligands **L**¹ and **L**².

We have previously reported that the reaction of **L**¹ with different copper(II) salts yields a series of infinite coordination networks whose structures are highly dependant on the counteranions present in solution.⁵⁸ Based on our previous results, we hypothesized that these relatively flexible ligands could be coordinated to metal complexes with restricted coordination sites to yield metallo-macrocycles the structures of which could be influenced by the presence of different anions. The results of these investigations using *cis*-[Pd(P–P)]²⁺ (where P–P is a chelating phosphine) are herein presented.

Results and discussion

Syntheses of ligands and structural characterisation of **L**¹

The bis-pyridyl compound **L**¹ was prepared by modification of the previously reported synthetic procedure,⁵⁹ using 1,1'-bisimidazole instead of diphenyl carbonate to generate the urea (see Experimental). Ligand **L**² had also been previously reported and was prepared using the literature procedure.⁶⁰ Both compounds were characterized spectroscopically and compared to the data previously reported.

Single crystals of **L**¹ suitable for X-ray crystallography were obtained from CH₂Cl₂. Interestingly, two different crystal structures were obtained, a solvent free (**L**^{1a}) and a monohydrate (**L**^{1b}). In both cases the structure shows **L**¹ to have a *cis*-geometry around the urea group. In the solvent-free crystal (**L**^{1a}) the structure contains two half independent molecules of **L**¹ which pack together in the centro-symmetrical space group *Pccn* (the two independent molecules have a crystallographically imposed two-fold symmetry with the central C=O bonds on two-fold axes). On the other hand in **L**^{1b} half molecules of **L**¹ pack in the chiral space group *P2₁2₁2₁*; the molecule has crystallographically-imposed twofold symmetry, with the central C=O bond on the twofold axes. The water molecule also lies on a twofold axis. In both structures, the **L**¹ molecules are connected *via* NH...O=C hydrogen bonds generating infinite chains (see Fig. 2 and Fig. 3). In **L**^{1a} the relative orientation of the inter-connected molecules is dictated by a rotation of 35.5° of the planes defined by the urea groups (see Fig. 2). The orientation of the pyridine rings in neighboring molecules is inverted giving rise to a staggered arrangement. In contrast, in **L**^{1b} the hydrogen-bonding urea groups of the connecting molecules are on the same plane defining the relative orientation of the molecules. The pyridine rings from neighboring molecules are perfectly stacked as shown in Fig. 3.

Although some previous structural studies on the co-crystallization of **L**¹ with other species (such as diiodopolynes and ureylene dicarboxylic acid)^{61,62} have been reported, this is the first time that the crystal structure of a pure sample of **L**¹ is reported.

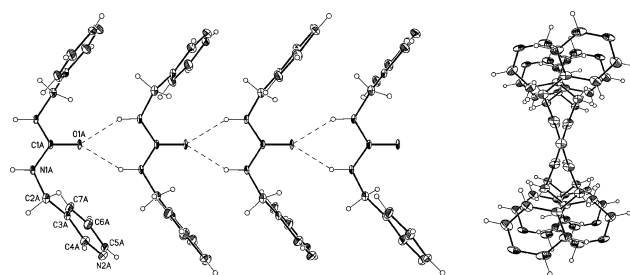


Fig. 2 Ortep-Plot (thermal ellipsoids shown at 50% probability level) of **L**^{1a} (only molecule A is shown) showing the NH...O=C hydrogen bonding. Distances: O1AA...N1AB: 2.877(6) Å (O1AA...H1AB: 2.09 Å uncorrected) and O1BA...N2BB: 2.868(6) Å (O1BA...H2BB: 2.09 Å uncorrected).

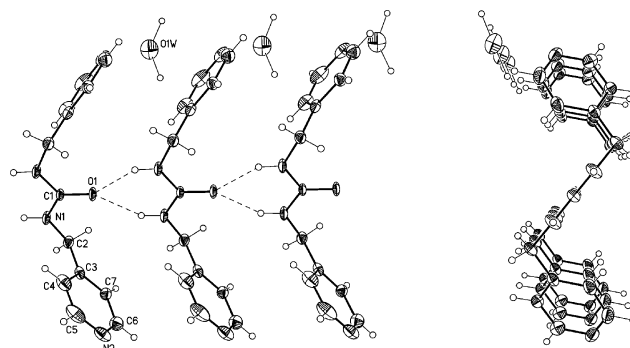


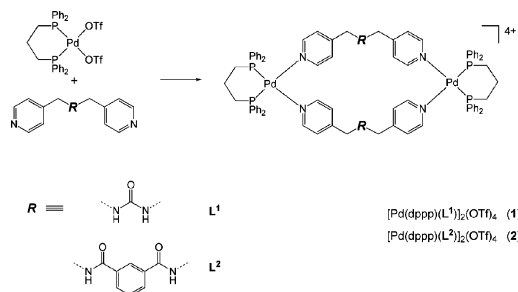
Fig. 3 Ortep-Plot (thermal ellipsoids shown at 50% probability level) of **L**^{1b} showing the NH...O=C hydrogen bonding. Distances: O1A...N1B: 2.866(6) Å (O1A...H1B: 2.07 Å uncorrected).

Synthesis and crystal structures of metalla-macrocycles [Pd(P–P)(**L**ⁿ)₂][OTf]₄

Once the ligands (**L**¹ and **L**²) had been prepared and fully characterized, their reactions with palladium(II) complexes were investigated. We first studied the products resulting from the reactions between [Pd(dppp)(OTf)₂] (prepared from [Pd(dppp)Cl₂] and AgOTf) and the corresponding ligand (either **L**¹ or **L**²). The reactions were carried out in CH₂Cl₂ using a 1 : 1 palladium-to-ligand ratio. Upon addition of the corresponding ligand to the [Pd(dppp)(OTf)₂] solution, a color change from yellow to colorless and the appearance of a white precipitate was observed. The reaction mixtures were stirred for several hours to ensure that they had gone to completion. At this stage, the solvent was removed under reduced pressure and the resulting solids washed with hexane. The ³¹P{¹H} NMR spectra of both these solids indicated that only one phosphorous-containing species had been formed in each case. The product resulting from the reaction with **L**¹ had a δ of 10.1 ppm while that obtained with **L**² a δ of 7.1 ppm. To explore whether the presence of a different anion in the palladium(II) starting material would have an influence on the outcome of the reaction, we also investigated the reaction between [Pd(dppp)(PF₆)₂] and **L**¹. The product obtained from this reaction, had a very similar ³¹P NMR spectrum to the one resulting from the reaction between [Pd(dppp)(OTf)₂] and **L**¹ (δ_P = 10.8 ppm plus a signal corresponding to PF₆). In order to establish unambiguously the stoichiometry and molecular structure of these assemblies,

single crystals of the three complexes were obtained and analyzed by X-ray crystallography.

The molecular structures of these compounds in the solid state showed them to be the [2 + 2] assemblies $[\text{Pd}(\text{dppp})(\text{L}^1)]_2(\text{OTf})_4$ (**1**) and $[\text{Pd}(\text{dppp})(\text{L}^2)]_2(\text{OTf})_4$ (**2**) (see Scheme 1).



Scheme 1

In these two assemblies the palladium centers have a distorted square planar geometry with two *cis* positions occupied by the dppp ligand and the other two by the pyridyl groups of either L^1 (in complex **1**—see Fig. 4) or L^2 (in complex **2**—see Fig. 5).

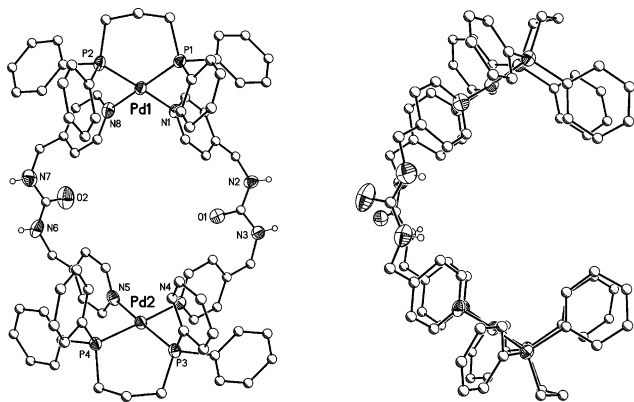


Fig. 4 Molecular structure of **1** (atoms in Ortep-plot: thermal ellipsoids shown at 50% probability level). The triflate counter-anions and non relevant hydrogen atoms have been omitted for clarity. Selected bond distances (Å) and angles (°): Pd1–N1: 2.108(4), Pd1–N8: 2.106(5), Pd1–P1: 2.2710(14), Pd1–P2: 2.2791(13), N1–Pd1–N8: 85.78(19), Pd2–N4: 2.089(4), Pd2–N5: 2.110(5), Pd2–P3: 2.2745(14), Pd2–P4: 2.2740(13) and N4–Pd2–N5: 86.07(17).

The N–Pd–N angles are contracted to 85.78(19)°/86.07(17)° in **1** and 86.2(3)°/86.1(3)° in **2**; this deviation from an ideal square planar geometry is likely to be a consequence of the geometrical arrangement of the corresponding ligands when the [2 + 2] assembly forms. The CH_2 groups that link the pyridyls to the central urea or diamide groups in L^1 and L^2 respectively allow for a good degree of flexibility in these ligands. As a consequence, the bridging molecules are bent giving a bowl-like geometry to the Pd_2L_2 cores in both **1** and **2** (see side view in Fig. 4, Fig. 5). This is more pronounced in the case of **2** where the planes formed by the coordination geometry around the two palladium centers are nearly parallel (with a $\text{Pd} \cdots \text{Pd}$ distance of approx. 10.5 Å).⁶³

In complex **1**, the carbonyl groups of the ureas are pointing to an isopropanol molecule which is located at the base of the molecule between the urea groups. The NH groups of the ureas

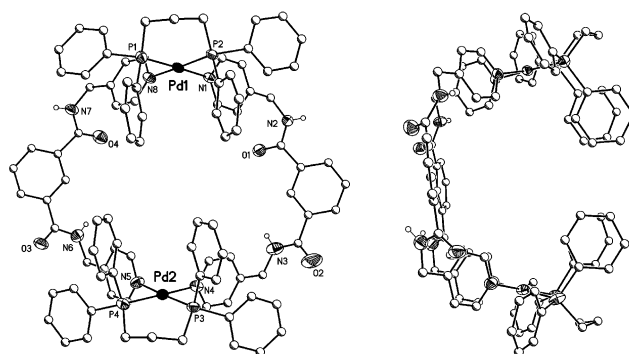


Fig. 5 Molecular structure of **2** (atoms in Ortep-plot: thermal ellipsoids shown at 50% probability level). The triflate counter-anions and non relevant hydrogen atoms have been omitted for clarity. Selected bond distances (Å) and angles (°): Pd1–N1: 2.095(6), Pd1–N8: 2.117(6), Pd1–P1: 2.273 (2), Pd1–P2: 2.264(2), N1–Pd1–N8: 86.2(2), Pd2–N4: 2.086(7), Pd2–N5: 2.094(7), Pd2–P3: 2.269(2), Pd2–P4: 2.270(2) and N4–Pd2–N5: 86.1(3).

form hydrogen bonds with two different triflate anions located at the sides of the metallo-macrocycle. The distances between the oxygen atoms of the triflate anions and the nitrogen atoms of the urea groups are in the region 2.8–2.9 Å. A third triflate anion is located in the middle of the assembly displaying weak interactions to different adjacent aromatic rings. The fourth triflate anion is located outside the “cavity” formed by the macrocycle at a relatively short distance from Pd2 (shortest distance $\text{Pd2} \cdots \text{O1B}$: 3.24 Å). In the crystal packing intermolecular interactions between urea groups cannot be observed.

The crystal structure of **2** (with ligand L^2) shows one of the triflate counter-anions located at the centre of the [2 + 2] assembly while two more are found at the sides of the metallo-macrocycle each of them interacting with one palladium center. The shortest distances between the counter-anions and the palladium atoms are: $\text{Pd1} \cdots \text{O2SA}$: 2.97 Å and $\text{Pd2} \cdots \text{O2SB}$: 2.98 Å. Further intermolecular interactions are found in this structure, in the crystal packing a combination of π – π and hydrogen bonding interactions between ligands of neighboring molecules can be found. These interactions lead to the formations of pairs of molecules as is shown in Fig. 6.

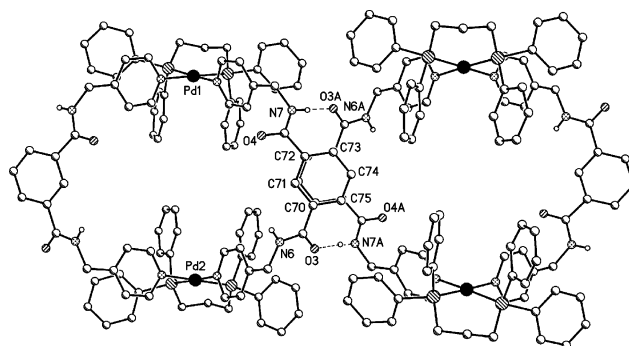


Fig. 6 Hydrogen bonding and π – π interactions between two molecules of **2**. The triflate anions, solvent molecules and non relevant hydrogen atoms have been omitted for clarity. Letter “A” in labelled atoms indicates that these are at equivalent positions ($-x, 1-y, 1-z$).

The distance of the observed hydrogen bond between the amides of L^2 is $O3 \cdots N7A$: 2.836(10) Å ($O3 \cdots H7A$: 1.99 Å uncorrected) and the distance between the planes of the aromatics rings (C70–C75) is *ca.* 3.7 Å. The second L^2 ligand (which is not engaged in hydrogen bonding) from each metallo-macrocycle, is packing between the described pairs forming stacks of molecules. The π – π distance in this case is of 4.90 Å too long to be considered a strong intermolecular interaction. Due to the stacking of the metallo-macrocycles, channels are formed in the crystal packing (see Fig. 7). The channels contain triflate counter-anions and partially disordered isopropanol molecules.

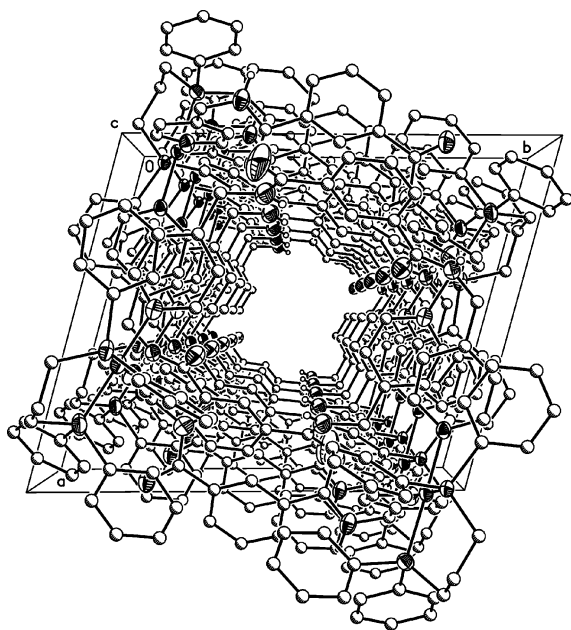


Fig. 7 Crystal packing of **2** with view along the *a*-axis showing the observed channel in the crystal array. The triflate counter-anions, solvent molecules and hydrogen atoms have been omitted for clarity.

In order to investigate whether the nature of the chelating phosphine could have an influence on the structure of the metallo-macrocycle formed, the reaction between $[Pd(dppf)(OTf)_2]$ (*dppf* = 1,1-*bis*(diphenylphosphino)ferrocene) and L^1 was carried out. As in the synthesis of **1** and **2**, a solid was isolated from the reaction mixture (see Experimental section) which, based on its analytical and spectroscopic characterisation, was formulated as $[Pd(dppf)(L^1)]_n(OTf)_{2n}$. In the ^{31}P NMR spectrum, a singlet at 32.7 ppm was observed while the elemental analyses were consistent with a Pd : *dppf* : L ratio of 1 : 1 : 1. To determine the nuclearity of this assembly, single crystals suitable for an X-ray crystallographic analysis were grown from an acetone–isopropanol mixture. As for the previous molecules, this compound was shown to be the [2 + 2] metallo-macrocycle $[Pd(dppf)(L^1)]_2(OTf)_4$ (**3**). The overall structure of **3** is very similar to that of **1**. The geometry around the palladium centers is also a distorted square planar with an N–Pd–N angle of 85.8°. As in the other two structures, the bridging ligands in **3** are bent giving a bowl-like structure with one of the triflates located at the center of the assembly (see Fig. 8). A second triflate interacts *via* hydrogen bonds with one of the urea groups ($O1D \cdots N6$: 2.907(7) Å ($O1D \cdots H6C$: 2.09 Å uncorrected) and $O2D \cdots N7$:

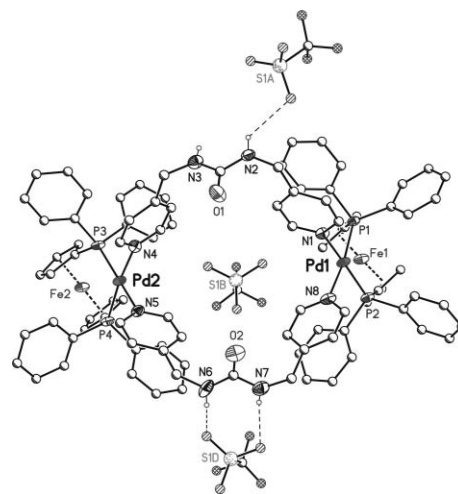


Fig. 8 Molecular structure of **3** (atoms in Ortep-plot: thermal ellipsoids shown at 50% probability level) showing the interaction with the triflate counter-anions. The fourth counter-anion, the solvent molecules and non relevant hydrogen atoms have been omitted for clarity. Selected bond distances and angles: Pd1–N1: 2.088(6), Pd1–N8: 2.096(6), Pd1–P1: 2.3057(19), Pd1–P2: 2.3102(17), N1–Pd1–N8: 85.8(2)°, Pd2–N4: 2.106(6), Pd2–N5: 2.104(6), Pd2–P3: 2.2984(18), Pd2–P4: 2.3030(19) and N4–Pd2–N5: 84.7(3).

2.971(7) Å ($O2D \cdots H7A$: 2.10 Å uncorrected). A third triflate is interacting partially with the second urea group, $O3A \cdots N2$: 3.117(7) Å ($O3A \cdots H2B$: 2.47 Å uncorrected) and weakly with one of the palladium atoms (Pd1 \cdots O2A: 4.16 Å). The fourth counter-anion is packing in the intermolecular area. Interactions between urea groups were not observed in this case.

The X-ray crystal structures of these four metallo-macrocycles indicate that, in the solid state, the geometrical constraints imposed by both the bis-pyridyl ligands and by the *cis*-square planar coordination around the palladium(II) centers favor the formation of [2 + 2] assemblies. However, in solution it would not be surprising that other species were present in equilibrium with the [2 + 2] assemblies. In order to investigate this possibility, we engaged in a detailed study of the behavior of **1** in solution.

Solution studies of $[Pd(dppp)(L^1)]_2[OTf]_4$ (**1**)

As indicated above, the $^{31}P\{^1H\}$ NMR spectrum of **1** showed only one singlet at 10.1 ppm which is consistent with the X-ray crystal structure of this compound. However, careful inspection of the 1H NMR spectrum in different solvents suggested a more complex behavior of this assembly in solution. When the 1H NMR spectrum was recorded in d_6 -DMSO (see Fig. 9, spectrum at the top) the signals were considerably broadened. Furthermore, a set of small signals could be seen next to some of the main resonances associated with the ligand. Interestingly, when the 1H NMR spectrum of the same sample of **1** was recorded in d_6 -acetone (see Fig. 9, spectrum at the bottom), sharp and well defined signals were obtained, and no “extra” peaks were present.

It was hence of interest to investigate further the behavior of the system in DMSO. First, a variable temperature 1H NMR experiment between 300 and 350 K was carried out. As can be seen in Fig. 10, upon increasing the temperature of **1** in d_6 -DMSO

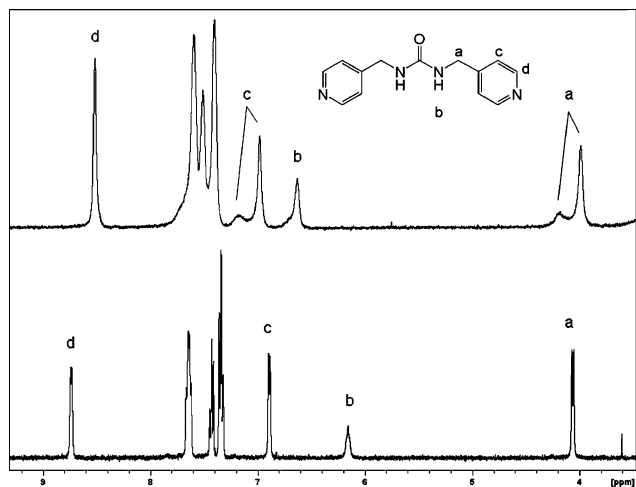


Fig. 9 Section of the ^1H NMR spectra of complex **1** in d_6 -DMSO (top) and d_6 -acetone (bottom). The structure of the ligand is shown to assign labels (although the spectra are of the metallo-assembly **1**).

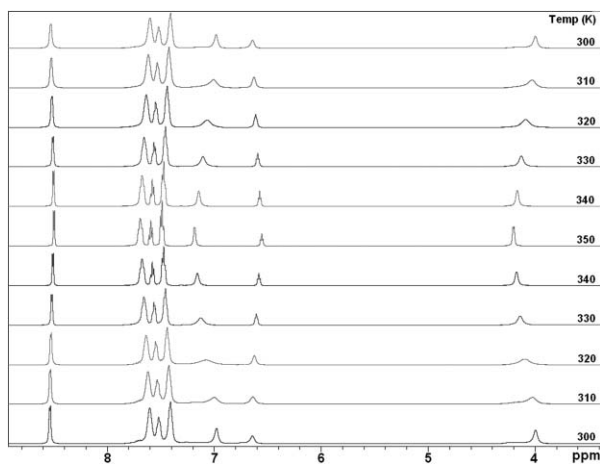


Fig. 10 Section of the ^1H NMR spectrum of palladium complex **1** in d_6 -DMSO at different temperatures ranging between 300 and 350 K.

two phenomena take place: sharpening of the signals and a shift of some of the signals (those associated to H_a , H_b and H_c —see labels in Fig. 9). To check that no decomposition of the assembly took place, the mixture was cooled down to the original temperature (300 K) and the ^1H and ^{31}P NMR spectra recorded again. Both of these spectra showed the product to be identical to the one at the beginning of the experiment.

The sharpening of the signals upon increasing the temperature of the solution could be associated to different dynamic processes. It could be possible that different conformations of the complex are in intermediate exchange in DMSO solution giving rise to the broadening and splitting of some of the proton signals (especially those associated to the NH and CH_2 groups). Upon increasing the temperature the conformational exchange becomes fast in the NMR timescale and produces a ^1H -NMR spectrum with just a single set of sharper signals. Another possible scenario is that the chemical exchange is taking place between supramolecular assemblies of different stoichiometry (e.g. a mixture of the [2 + 2] and [3 + 3] metallo-macrocycles).⁶⁴

To elucidate which one of the two phenomena outlined above was responsible for the spectroscopic behavior observed, a ^1H NMR dilution experiment of **1** in d_6 -DMSO was carried out.⁶⁵ As can be seen in Fig. 11, upon reducing the concentration of **1** in d_6 -DMSO no important shifts of the resonances were detected. However, a clear change in the relative integration of the pairs of signals associated to H_a and H_c can be seen (presumably a similar change takes place for H_b however this signal and its “pair” are too broad to be independently identified). This change is most apparent if the first and last spectra are compared.

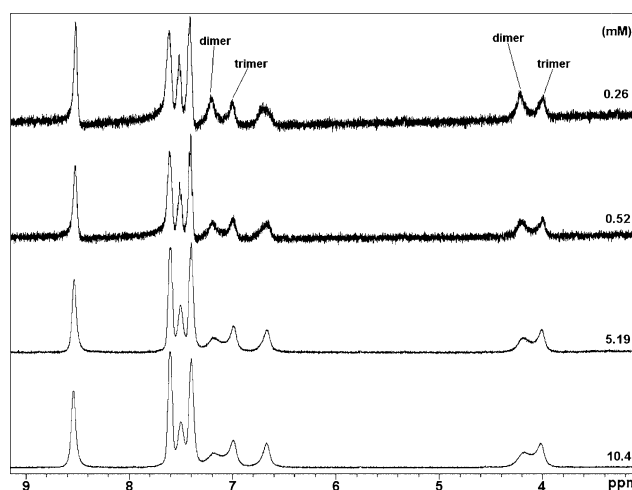


Fig. 11 Section of the ^1H NMR spectrum of **1** in d_6 -DMSO at different concentrations ranging between 10.40 and 0.26 mM.

The fact that the relative integrations of the pairs of peaks change at different concentrations indicates the presence of assemblies with different stoichiometry rather than different conformations of the complex. As indicated above, a likely explanation is that two or more assemblies with different nuclearities—presumably the [2 + 2] and [3 + 3] metallo-macrocycles—are present in DMSO. From an entropic point of view, the smaller assembly (i.e. the [2 + 2] species) should form at higher temperatures and at lower concentrations. With this in mind, we have assigned in the ^1H NMR spectra of Fig. 11 the proton signals corresponding to the lower nuclearity assembly (i.e. the [2 + 2]) and those for a higher nuclearity species (hypothetically the [3 + 3]).

To investigate whether the [3 + 3] metallo-assembly was indeed present, a high resolution ESI mass spectrum of **1** was recorded. It should be noted that the solvent employed to dissolve the sample and record the mass spectrum was acetonitrile and not DMSO, which was the solvent used in the NMR experiments described above. The mass spectrum was dominated by a peak at 909.3 amu which corresponds to $[\text{Pd}(\text{dppp})(\text{L}^1)(\text{OTf})]^+$. Closer inspection of the isotopic pattern of this peak, allowed us to identify lower intensity peaks of half mass-units which are indicative of the presence of a doubly charged species, i.e. $[\text{Pd}_2(\text{dppp})_2(\text{L}^1)_2(\text{OTf})_2]^{2+}$. A low intensity peak centered at 1439.19 amu with a complex isotopic pattern (see Fig. 12) was also present in the spectrum, the m/z and isotopic pattern of this peak are consistent with the formulation $[\text{Pd}_3(\text{dppp})_3(\text{L}^1)_3(\text{OTf})_4]^{2+}$ which suggests that the [3 + 3] assembly is indeed present in solution. The ESI mass spectrum did not provide evidence for the presence of a [4 + 4] macrocyclic species or any other higher nuclearity assemblies.

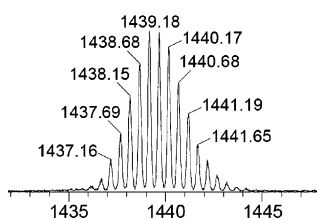
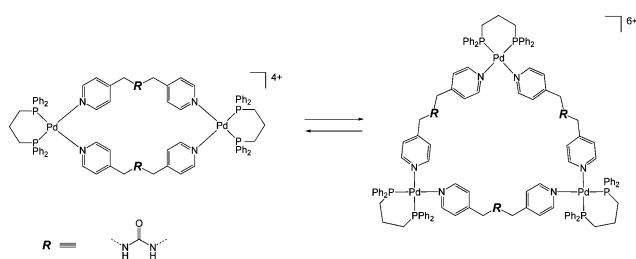


Fig. 12 Peak associated to $[\text{Pd}_3(\text{dppp})_3(\text{L}^1)_3(\text{OTf})_4]^{2+}$ in the high resolution ESI mass spectrum of a solution of $[\text{Pd}(\text{dppp})(\text{OTf})_2]$ plus L^1 (which yields **1** in the solid state but a mixture of products in solution).

In summary, the mass spectrometric evidence together with the ^1H NMR spectroscopic data, strongly suggest that in solution there is a dynamic equilibrium between the $[2 + 2]$ metallo-macrocycle **1** (which is also the one that crystallizes) and the $[3 + 3]$ metallo-macrocycle $[\text{Pd}_3(\text{dppp})_3(\text{L}^1)_3](\text{OTf})_6$ —see Scheme 2). This equilibrium is affected by the concentration, the solvent employed and the temperature of the solution.



Scheme 2

Anion binding studies of **1**

Our attention was then directed to establishing whether the addition of different anions would modify the distribution of products in the equilibrium described above. Therefore, a sample of **1** was dissolved in d_6 -DMSO giving the expected mixture of $[2 + 2]$ and $[3 + 3]$ assemblies (see previous section). Aliquots of this mixture were taken to carry out ^1H NMR titration experiments with different anions. As is shown in Fig. 13, addition of increasing amounts of $[\text{NBu}_4][\text{H}_2\text{PO}_4]$ to this solution caused interesting changes in the spectrum. Initially (up to *ca.* 3 equivalents of

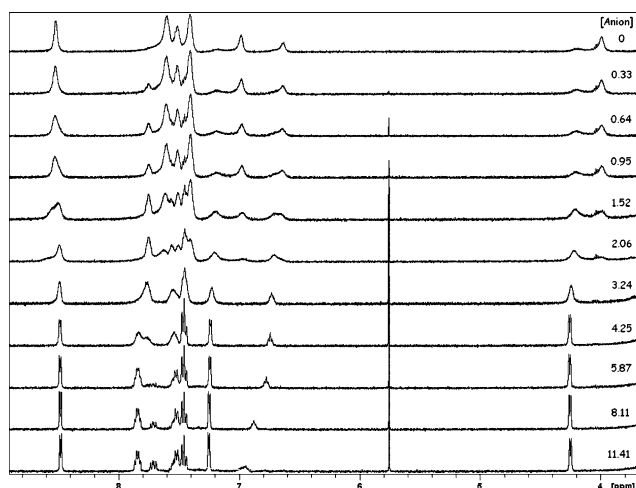


Fig. 13 Changes in the ^1H NMR spectra of **1** in DMSO upon addition of increasing amounts of $[\text{H}_2\text{PO}_4]^-$ (between 0 and 11.41 equivalents).

the anion) there are little changes in the chemical shifts of the signals, however, an important change in the relative integration between the signals assigned to the $[2 + 2]$ and $[3 + 3]$ assemblies can be seen. This observation indicates that the initial addition of $[\text{H}_2\text{PO}_4]^-$ modifies the equilibrium between the two assemblies favoring the formation of the $[2 + 2]$ macrocycle. This behavior is probably due to the selective binding of the $[\text{H}_2\text{PO}_4]^-$ anion with the $[2 + 2]$ assembly with a concomitantly displacement of the equilibrium between “free” assemblies. Interestingly, once enough anion has been added (*ca.* 4 equivalents) to displace almost completely the equilibria to the formation of $[2 + 2]$ assembly, a second phenomenon is observed. That is, the addition of more than 4 equivalents of $[\text{H}_2\text{PO}_4]^-$ anion sharpen the proton signals and the NH signal of the urea shifts slightly to lower field. These observations are consistent with the elimination of the slow chemical exchange previously operative between “free” assemblies and responsible for the broadening of the signals together with the complex formation between the remaining free $[2 + 2]$ assembly, at this point of the titration, and the anion being added.

Interestingly, when the analogous titration experiment was repeated with $[\text{NBu}_4][\text{HSO}_4]$ a different behavior was observed (see Fig. 14). Even after addition of *ca.* 12 equivalents of the anion, no important changes were observed in the relative integration of the peaks associated to the two different assemblies (*i.e.* the $[2 + 2]$ and $[3 + 3]$ macrocycles) present in solution. However, a shift of some of the signals can be clearly seen which suggests that the added $[\text{HSO}_4]^-$ binds selectively to the $[3 + 3]$ metallo-host. In this case, the extent of the binding has not displaced completely the equilibrium towards the $[3 + 3]$ assembly since the signals of the $[2 + 2]$ assembly are still visible in the ^1H NMR spectra. Likewise, the chemical equilibrium between free metallo-macrocycles is still operative as can be inferred from the broadening of the proton signals.

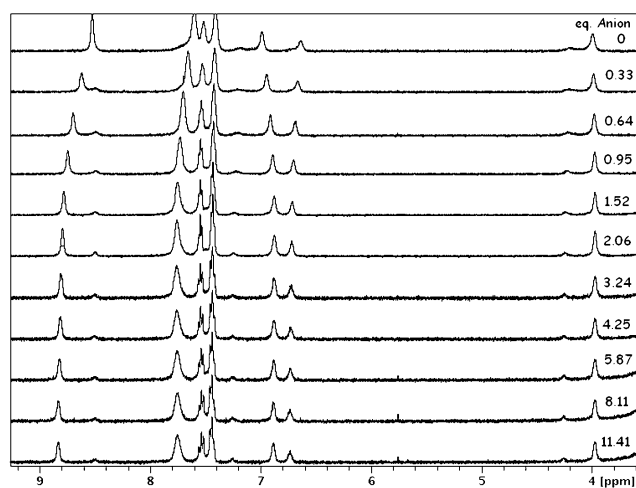
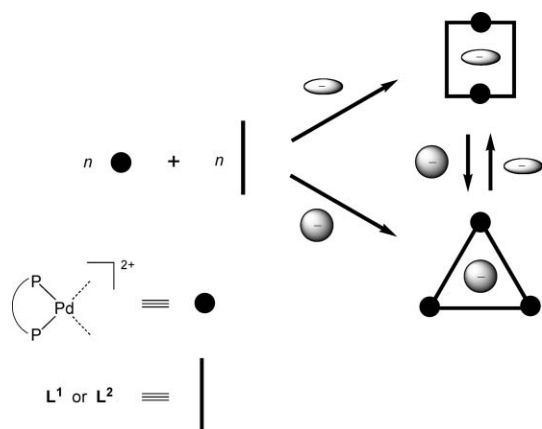


Fig. 14 Changes in the ^1H NMR spectra of **1** in DMSO upon addition of increasing amounts of $[\text{HSO}_4]^-$ (between 0 and 11.41 equivalents).

Addition of di-carboxylates such as oxalate and malonate, had a similar effect to the one observed with $[\text{H}_2\text{PO}_4]^-$ *i.e.* the equilibrium is shifted to the formation of the $[2 + 2]$ macrocycle.

Taken together, these results suggest the possibility of using different anions to template the formation of metallo-macrocycle of different sizes and stoichiometry (see Scheme 3). To confirm



Scheme 3 Schematic representation of the effect of different anions in the equilibrium between two metallo-macrocycles (square/triangle).

this hypothesis, several attempts to grow crystals from a mixture containing $[\text{Pd}(\text{dppp})(\text{OTf})_2]$, L^1 and $[\text{HSO}_4]^-$ were carried out with the hope to isolate in the solid state a $[3 + 3]$ metallo-macrocycle. Unfortunately, to date this has been unsuccessful and further studies will be required to characterize the $[3 + 3]$ macrocycle in the solid state.

Conclusions

Three different $[2 + 2]$ metallo-macrocycles (**1–3**) based on flexible bis-pyridyl ligands containing hydrogen bonding groups have been successfully prepared and structurally characterized. In the solid state, these species have a bowl-type structure allowing, in some cases, for the encapsulation of anionic species *via* a combination of several weak supramolecular interactions. Detailed ^1H NMR spectroscopic solution studies for **1** have been carried out showing that in DMSO this species is in a dynamic equilibrium with a larger assembly (likely to be the $[3 + 3]$ metallo-macrocycle). The equilibrium between these two species can be modified by changing the temperature, the concentration, the solvent or by addition of different anions. Although at the moment the system gives rise to only two different assemblies, it is expected that in the presence of a mixture of ligands a larger library of metallo-macrocycles could be obtained. Studies are currently underway to develop this type of library and study whether the addition of different anions will allow amplification of a specific metallo-assembly.

Experimental

General

All experimental procedures were carried out using standard high vacuum and Schlenk-line techniques under an atmosphere of dry nitrogen or argon. Glassware was dried in an oven at 150°C prior to use. ^1H , ^{13}C and ^{31}P NMR spectra were recorded on a Bruker Avance 400 or Bruker Avance 500 spectrometers and referenced to residual ^1H and ^{13}C signals of the solvents or 85% H_3PO_4 as an external standard (^{31}P). The high resolution ESI mass spectrometric results (see Fig. 12 and mass spectrum in the ESI†) were obtained at the University of London School of Pharmacy. The sample was run in acetonitrile on a Waters QTOF Global Ultima, positive ion mode, *v*-mode using borosilicate tips (direct

infusion). Capillary voltage 1.8 kV, cone 100 V and collision energy set to 10 eV. $[\text{Pd}(\text{dppp})\text{Cl}_2]$, $[\text{Pd}(\text{dppf})\text{Cl}_2]$ and L^2 were synthesized following literature procedures.^{60,66,67}

Synthesis of $\text{N,N}'\text{-(C}_5\text{H}_4\text{N-}p\text{-CH}_2\text{)}_2\text{-NHC(=O)NH (L}^1\text{)}$

A slight modification of a reported method by Fowler⁵⁹ was used: 1,1'-carbonyldiimidazole (0.689 g, 4.3 mmol) was dissolved in CH_2Cl_2 (30 ml) under an argon atmosphere. 4-Picolylamine (0.89 ml, 8.6 mmol) was added slowly into the solution and the reaction was stirred at 40°C for 20 h. The volume was then reduced to *ca.* 10 ml under reduced pressure and ethyl acetate (50 ml) was added to precipitate the crude product. The solid formed was filtered, washed with ethyl acetate (2×10 ml) and air dried to produce the final product as a white powder. Yield: 0.518 g, 50%. Mp = $185\text{--}186^\circ\text{C}$ (mp reported by Fowler and co-workers = $186\text{--}187^\circ\text{C}$). IR (ν (KBr)): 3335 (N–H), 3024 (aromatic C–H), 2934 (aliphatic C–H), 1628 (C=O). ^1H NMR (dms- d_6) δ (in ppm) = 8.49 (dd, 4H, 2-PyH, $^3J_{\text{H-H}} = 4.4$ Hz, $^4J_{\text{H-H}} = 1.7$ Hz), 7.24 (dd, 4H, 3-PyH, $^3J_{\text{H-H}} = 4.4$ Hz, $^4J_{\text{H-H}} = 1.7$ Hz), 6.74 (t, 2H, NH, $^3J_{\text{NH-CH}} = 6.1$ Hz), 4.26 (d, 4H, SCH_2 , $^3J_{\text{NH-CH}} = 6.1$ Hz). ^{13}C NMR (dms- d_6) δ (in ppm) = 158.1 (C=O), 149.4 (2-Py), 121.9 (3-Py), 42.0 (CH_2).

Synthesis of $[(\text{dppp})\text{Pd}(\mu\text{-L}^1)]_2[\text{SO}_3\text{CF}_3]_4$ (**1**)

$[\text{Pd}(\text{dppp})\text{Cl}_2]$ (0.089 g, 0.15 mmol) and AgSO_3CF_3 (0.077 g, 0.30 mmol) were dissolved in CH_2Cl_2 (20 ml) and stirred in an inert atmosphere of N_2 and in the absence of light for 72 h at room temperature. After this time the reaction was filtered to remove the precipitate of AgCl and the resulting yellowish solution of $[(\text{dppp})\text{Pd}(\text{CF}_3\text{SO}_2)]$ was used in the following step without further purification. To this solution ligand L^1 (0.036 g, 0.15 mmol) was added as a solid. Almost immediately the yellow solution became colorless and a white precipitate started appearing. The mixture was left stirring at room temperature overnight under N_2 . After this time the mixture was filtered off recovering a white solid that was washed with *n*-pentane and dried under reduced pressure at *ca.* 100°C . Yield: 0.086 g, 54% (with respect to palladium). Elemental Analysis Found: C, 47.36; H, 3.77; N, 5.14. Calculated for $\text{C}_{88}\text{H}_{80}\text{F}_{12}\text{N}_8\text{O}_{14}\text{P}_4\text{Pd}_2\text{S}_4$: C, 47.62; H, 3.81; N, 5.29. IR (ν (KBr)): 3395 (N–H), 3059 (aromatic C–H), 2925 (aliphatic C–H), 1665, 1618 (C=O), 1571, 1437, 1256, 1161, 1030 (CF_3SO_3^-). FAB(+)-MS m/z (in amu): 1727 (2%), $[\text{Pd}_2(\text{dppp})_2(\text{L}^1)(\text{CF}_3\text{SO}_3)_3]^+$; 759 (2%), $[\text{Pd}(\text{dppp})(\text{L}^1)]^+$; 667 (100%), $[\text{Pd}(\text{dppp})(\text{CF}_3\text{SO}_3)]^+$ (for the results obtained using ESI(+)-MS see Results and Discussion section). ^{31}P NMR (acetone- d_6) δ = 10.1 ppm. ^1H NMR (acetone- d_6) δ (in ppm) = 8.88 (d, 8H, 2-PyH, $^3J_{\text{H-H}} = 5.6$ Hz), 7.79 (m, 16H, *o*-ArH(dppp)), 7.57 (m, 8H, *p*-ArH(dppp)), 7.49 (m, 16H, *m*-ArH(dppp)), 7.03 (d, 8H, 3-PyH, $^3J_{\text{H-H}} = 5.6$ Hz), 6.32 (broad, 4H, NH), 4.20 (d, 8H, CH_2NH , $^3J_{\text{NH-CH}} = 5.7$ Hz), 3.41 (broad, 8H, CH_2P), 2.41 (broad, 4H, $\text{CH}_2\text{CH}_2\text{P}$). ^{19}F NMR (acetone- d_6) δ (in ppm) = -78.8 . Crystals suitable for X-ray analysis were obtained by slow evaporation from an acetone–isopropanol solution.

Synthesis of $[(\text{dppp})\text{Pd}(\mu\text{-L}^2)]_2(\text{SO}_3\text{CF}_3)_4$ (**2**)

$\text{Pd}(\text{dppp})\text{Cl}_2$ (102.1 mg, 0.1466 mmol) was dissolved in *ca.* 20 mL of CH_2Cl_2 . To this solution, AgCF_3SO_3 (81.7 mg, 0.3180 mmol) was added as a solid. The mixture was left stirring at room temperature for 72 h with exclusion of light. After this time, the

reaction was filtered to remove AgCl and the yellowish solution used in the following step without further purification. To this yellow solution ligand **L**² (52 mg, 0.1468 mmol) was added as a solid. Almost immediately after addition, the yellow color of the solution disappeared yielding a colorless solution and some white precipitate. The reaction mixture was left stirring overnight after which time it was filtered and the solvent was evaporated to dryness under reduced pressure. This solid was washed with *n*-pentane and dried under reduced pressure at *ca.* 100 °C. Yield: 125.1 mg, 73% (with respect to palladium). Elemental Analysis Found: C, 50.50; H, 3.76; N, 4.85. Calculated for C₉₈H₈₈N₈O₁₆S₄F₁₂P₄Pd₂: C, 50.52; H, 3.78; N, 4.81. IR (ν (KBr)): 3439 (N–H), 3057 (aromatic C–H), 2926 (aliphatic C–H), 1668, 1618 (C=O), 841 (PF₆[−]). ³¹P NMR (CD₃CN) δ = 7.1 ppm. ¹H NMR (acetone-d₆) δ (in ppm) = 8.45 (d, ³J_{HH} = 6 Hz, 8H, py), 8.25 (broad singlet, 2H, Ph), 7.95 (dd, ³J_{HH} = 6 Hz, ⁴J_{HH} = 2 Hz, 4H, Ph), 7.75 (m, 43H, Ph), 7.60–7.28 (broad, 4H, NH), 7.13 (broad, 8H, py), 4.41 (broad, 8H, –CH₂–py), 3.05 (broad, 8H, –CH₂CH₂ dppp), 2.1 (broad, –CH₂–dppp). ¹⁹F NMR (acetone-d₆) δ (in ppm) = –78.1 ppm. Crystals suitable for X-ray crystallography were obtained from isopropanol.

Synthesis of [(dppf)Pd(μ -L¹)]₂(SO₃CF₃)₄ (**3**)

Pd(dppf)Cl₂ (50 mg, 0.0612 mmol) was dissolved in *ca.* 20 mL of dry and degassed CH₂Cl₂. To this solution, AgSO₃CF₃ (37 mg, 0.1440 mmol) was added as a solid. The mixture was left stirring at room temperature for 72 h with exclusion of light. After this time, the reaction was filtered to remove AgCl and the resulting dark green solution was used in the following step without further purification. To the solution containing Pd(dppf)(SO₃CF₃)₂ ligand **L**¹ (15.1 mg, 0.0624 mmol) was added as a solid under vigorous stirring. Almost immediately after addition the dark green color changed to purple. The mixture was left stirring at room temperature overnight after which time it was filtered to remove a white solid precipitate (which ¹H NMR showed was some unreacted ligand). The purple solution was concentrated to *ca.* 2 mL and diethyl ether was added to yield a purple solid. The solid was recovered and dried under reduced pressure overnight heating at *ca.* 100 °C. Yield: 21.1 mg, 20% (with respect to palladium). Elemental Analysis Found: C, 49.10; H, 3.59; N, 4.80. Calculated for C₉₈H₈₄N₈O₁₄P₄F₁₂S₄Fe₂Pd₂: C, 48.97; H, 3.50; N, 4.66. IR (ν (KBr)): 3396 (N–H), 3098 (aromatic C–H), 2925 (aliphatic C–H), 1670, 1618 (C=O), 1554, 1436, 1257, 1224, 1165, 1097, 1062, 1030 (CF₃SO₃[−]), 749, 696, 638, 556, 516, 494, 467. ³¹P NMR (CD₂Cl₂) δ = 32.70 ppm. ¹⁹F NMR (CD₂Cl₂) δ (in ppm) = –80.8 ppm. Crystals suitable for X-ray analysis were obtained from an acetone–isopropanol solution (by slow evaporation).

X-Ray structure determination

Crystals of **1**, **2** and **3** were obtained by crystallisation in isopropanol (**1** and **2**) and dichloromethane (**3**). Crystals were generally of poor quality and with the tendency of degradation due to solvent losses. The measured crystals were quickly prepared under inert conditions immersed in perfluoropolyether as protecting oil for manipulation. Measurements were made on a Bruker-Nonius diffractometer equipped with a APPEX 2 4K CCD area detector, a FR591 rotating anode with Mo-K α radiation, Montel mirrors as monochromator and a Kryoflex low temperature device (*T* =

–173 °C). Full-sphere data collection was used with ω and φ scans. Programs used: Data collection Apex2 V. 1.0–22 (Bruker-Nonius 2004), data reduction *Saint+* Version 6.22 (Bruker-Nonius 2001) and absorption correction SADABS V. 2.10 (2003). The structure solution and refinement was carried out using *SHELXTL* Version 6.10 (Sheldrick, 2000).⁶⁸

CCDC reference numbers 624779–62478 and 624783–624784.

For crystallographic data in CIF or other electronic format see DOI: 10.1039/b703660d

Crystal data for L¹a at 100 K. C₁₃H₁₄N₄O₁, 242.28 g mol^{−1}, orthorhombic, *Pccn*, *a* = 16.291(2) Å, *b* = 16.300(2) Å, *c* = 9.1949(12) Å, *V* = 2441.7(6) Å³, *Z* = 8, ρ_{calcd} = 1.318 Mg m^{−3}, *R*₁ = 0.0634 (0.0700), *wR*₂ = 0.1827 (0.1901), for 4197 reflections with *I* > 2 σ (*I*) (for 4673 reflections [*R*_{int}: 0.0619] with a total measured of 16 300 reflections), goodness-of-fit on *F*² = 1.058, largest diff. peak (hole) = 0.488 (−0.278) e Å^{−3}.

Crystal data for L¹b at 100 K. C₁₃H₁₄N₄O₁·H₂O, 260.30 g mol^{−1}, orthorhombic, *P2₁2₁2₁*, *a* = 10.5821(18) Å, *b* = 13.149(3) Å, *c* = 4.5942(8) Å, *V* = 639.3(2) Å³, *Z* = 2, ρ_{calcd} = 1.352 Mg m^{−3}, *R*₁ = 0.0712 (0.0770), *wR*₂ = 0.2021 (0.2063), for 2989 reflections with *I* > 2 σ (*I*) (for 3252 reflections [*R*_{int}: 0.0292] with a total measured of 11 047 reflections), goodness-of-fit on *F*² = 1.175, largest diff. peak (hole) = 0.419 (−0.894) e Å^{−3}.

Crystal data for 1 at 100 K. C₈₀H₈₀N₈O₂P₄Pd₂·4C₁F₃O₃S₁·1·C₃H₈O₁, 2196.60 g mol^{−1}, orthorhombic, *P2₁2₁2₁*, *a* = 18.6063(11) Å, *b* = 21.5364(13) Å, *c* = 27.1103(16) Å, *V* = 10863.4(11) Å³, *Z* = 4, ρ_{calcd} = 1.343 Mg m^{−3}, *R*₁ = 0.0854 (0.1067), *wR*₂ = 0.2381 (0.2552), for 32 844 reflections with *I* > 2 σ (*I*) (for 41 344 reflections [*R*_{int}: 0.0501] with a total measured of 160 178 reflections), goodness-of-fit on *F*² = 1.091, largest diff. peak (hole) = 3.535(−2.093) e Å^{−3}. This structure refines as a racemic twin with ratio of 53 : 47. Crystals of this compound are highly sensitive to losing partially its solvent molecules. After refinement there are residual voids which are likely to contain not-localised highly-disordered isopropanol molecules. In general the triflate anions and specially the isopropanol molecules are disordered. The detected highest peak and deepest hole of the electron densities are localized close to one of the disordered sulfur atoms belonging to a triflate anion and could not be improved. Due to the high number of anions and localised solvent molecules contained in the crystal packing, it was considered better not to use *SQUEEZE*⁶⁹ for data improvement. Distances and thermal displacement parameters for these molecules were partially restrained.

Crystal data for 2 at 100 K. The crystals measured are of small dimensions and extremely sensitive to losing solvent. C₉₄H₈₈N₈O₄P₄Pd₂·4C₁F₃O₃S₁·3/4C₃H₈O₁·2H₂O (some of the hydrogen atoms could not be localised), 2404.26 g mol^{−1}, *P1*, *a* = 15.8443(7) Å, *b* = 18.8383(9) Å, *c* = 20.6983(8) Å, *a* = 95.680(2)°, β = 94.482(2)°, γ = 104.570(2)°, *V* = 5915.8(4) Å³, *Z* = 2, ρ_{calcd} = 1.350 Mg m^{−3}, *R*₁ = 0.0841 (0.1796), *wR*₂ = 0.2237 (0.2690), for 28010 reflections with *I* > 2 σ (*I*) (for 12 427 reflections [*R*_{int}: 0.1251] with a total measured of 74 819 reflections), goodness-of-fit on *F*² = 0.977, largest diff. peak (hole) = 2.424 (−1.143) e Å^{−3}. Similar to compound **1**, crystals of this compound are highly sensitive to losing partially solvent molecules. The triflate anions refined are partly disordered with large thermal ellipsoids. Also

the isopropanol and the water molecules localised are disordered and in some cases have partial assigned occupancies. Distances and thermal displacement parameters for these anions/solvent molecules are restrained. After final refinement there are residual voids which probably contain highly disordered isopropanol and water molecules which could not be clearly identified. The detected highest peak and deepest hole of the residual electron densities are localised close to one of the disordered solvent molecules but could not be identified and refined as disordered solvent. Applying *SQUEEZE* (Platon)⁶⁹ did not give significant data improvements resulting in similar *R*-values as modeling disordered solvent molecules.

Crystal data for 3 at 100 K. C₉₄H₈₄Fe₂N₈O₂P₄Pd₂·4C₁F₃O₃S₁·1C₁H₂Cl₂·3H₂O (without hydrogen atoms), 2535.28 g mol⁻¹, *P* $\bar{1}$, *a* = 15.828(3) Å, *b* = 16.901(3) Å, *c* = 20.704(8) Å, α = 71.936(4)°, β = 86.141(4)°, γ = 87.923(4)°, *Z* = 2, ρ_{calcd} = 1.603 Mg m⁻³, *R*₁ = 0.0973 (0.1402), *wR*₂ = 0.2504 (0.2967), for 25830 reflections with *I* > 2σ(*I*) (for 17 616 reflections [*R*_{int}: 0.0759] with a total measured of 55 822 reflections), goodness-of-fit on *F*² = 1.056, largest diff. peak (hole) = 2.889 (−2.727) e Å⁻³. The crystal contains disordered water molecules with partial assigned occupancies. The triflate counter-anions are also partly disordered and are showing large thermal displacement parameters.

Variable temperature ¹H-NMR experiments

Variable temperature NMR spectroscopy experiments of palladamacrocyclic **1** were carried out by dissolving ca. 2 mg of the complex in DMSO-*d*₆, under Ar. ¹H NMR spectra of this sample were recorded at increasing temperature at intervals of 10 K starting from 300 K up to 350 K and back again to the initial temperature. The ³¹P NMR spectra at initial (300 K), intermediate (350 K) and final (300 K) temperatures were also measured to verify complex integrity throughout the whole process.

¹H-NMR spectroscopic titrations of **1** with different anions

The following procedure is the one used for the titration with [H₂PO₄]⁻. An analogous procedure was used for all the other anions. All operations were carried out in an inert argon atmosphere. A host stock solution was prepared by dissolving **1** (4.1 mg, 0.002 mmol) in *d*₆-DMSO (2 ml). An aliquot of this solution (1.2 ml) was used to dissolve [NBu₄][H₂PO₄] (6.6 mg, 0.02 mmol) to prepare the guest stock solution employed for titrating the metallo-macrocycle. An initial aliquot (0.5 ml) of the host stock solution was transferred into an NMR tube and its ¹H-NMR spectrum determined. Increasing volumes of the guest stock solution were added with a micro-syringe into the same sample to reach, at the end, ca. 12 equivalents. The ¹H-NMR spectra of the sample after each addition were measured and the chemical shifts of the urea and aromatic protons recorded. The ³¹P NMR spectra of selected samples (including the initial and final points) were measured to confirm the integrity of the complex throughout the whole procedure.

References

- 1 S. R. Seidler and P. J. Stang, *Acc. Chem. Res.*, 2002, **35**, 972–983.
- 2 M. Fujita, *Struct. Bonding*, 2000, **96**, 177–201.
- 3 K. Biradha and M. Fujita, *Adv. Supramol. Chem.*, 2000, **6**, 1–39.

- 4 S. Leininger, B. Olenyuk and P. J. Stang, *Chem. Rev.*, 2000, **100**, 853–907.
- 5 M. Fujita, *Chem. Soc. Rev.*, 1998, **27**, 417–425.
- 6 J. A. R. Navarro and B. Lippert, *Coord. Chem. Rev.*, 2001, **222**, 219–250.
- 7 B. J. Holliday and C. A. Mirkin, *Angew. Chem., Int. Ed.*, 2001, **40**, 2022–2043.
- 8 M. Fujita, M. Tominaga, A. Hori and B. Therrien, *Acc. Chem. Res.*, 2005, **38**, 369–378.
- 9 D. Fiedler, D. H. Leung, R. G. Bergman and K. N. Raymond, *Acc. Chem. Res.*, 2005, **38**, 349–358.
- 10 M. Fujita, J. Yazaki and K. Ogura, *J. Am. Chem. Soc.*, 1990, **112**, 5645–5647.
- 11 Z. Qin, M. C. Jennings and R. J. Puddephatt, *Inorg. Chem.*, 2002, **41**, 3967–3974.
- 12 S.-S. Sun, J. A. Anspach, A. J. Lees and P. Y. Zavalij, *Organometallics*, 2002, **21**, 685–693.
- 13 F. Würthner and A. Sautter, *Chem. Commun.*, 2000, 445–446.
- 14 R. V. Slone, K. D. Benkstein, S. Belanger, J. T. Hupp, I. A. Guzei and A. L. Rheingold, *Coord. Chem. Rev.*, 1998, **171**, 221–243.
- 15 R. V. Slone, D. I. Yoon, R. M. Calhoun and J. T. Hupp, *J. Am. Chem. Soc.*, 1995, **117**, 11813–11814.
- 16 D. L. Caulder and K. N. Raymond, *Acc. Chem. Res.*, 1999, **32**, 975–982.
- 17 A. V. Davis, R. M. Yeh and K. N. Raymond, *Proc. Natl. Acad. Sci. USA*, 2002, **99**, 4793–4796.
- 18 R. W. Saalfrank and I. Bernt, *Curr. Opin. Solid State Mater. Sci.*, 1998, **3**, 407–413.
- 19 R. W. Saalfrank, E. Uller, B. Demleitner and I. Bernt, *Struct. Bonding*, 2000, **96**, 149–175.
- 20 R. W. Saalfrank and B. Demleitner, *Persp. Supramol. Chem.*, 1999, **5**, 1–51.
- 21 F. M. Raymo and J. F. Stoddart, *Templated Org. Synth.*, 2000, 75–104.
- 22 D. H. Busch, A. L. Vance and A. G. Kolchinski, *Comp. Supramol. Chem.*, 1996, **9**, 1–42.
- 23 S. Anderson, H. L. Anderson and J. K. M. Sanders, *Acc. Chem. Res.*, 1993, **26**, 469–475.
- 24 C. O. Dietrich-Buchecker and J. P. Sauvage, *Chem. Rev.*, 1987, **87**, 795–810.
- 25 S. J. Rowan, S. J. Cantrill, G. R. L. Cousins, J. K. M. Sanders and J. F. Stoddart, *Angew. Chem., Int. Ed.*, 2002, **41**, 899–952.
- 26 J.-M. Lehn and A. V. Eliseev, *Science*, 2001, **291**, 2331–2332.
- 27 G. R. L. Cousins, S.-A. Poulsen and J. K. M. Sanders, *Curr. Opin. Chem. Biol.*, 2000, **4**, 270–279.
- 28 P. T. Corbett, J. Leclaire, L. Vial, K. R. West, J.-L. Wietor, J. K. M. Sanders and S. Otto, *Chem. Rev.*, 2006, **106**, 3652–3711.
- 29 R. Vilar, *Angew. Chem., Int. Ed.*, 2003, **42**, 1460–1477.
- 30 P. D. Beer and P. A. Gale, *Angew. Chem., Int. Ed.*, 2001, **40**, 486–516.
- 31 S. Otto and S. Kubik, *J. Am. Chem. Soc.*, 2003, **125**, 7804–7805.
- 32 B. Hasenknopf, J.-M. Lehn, N. Boumediene, A. Dupont-Gervais, A. Van Dorsselaer, B. Kneisel and D. Fenske, *J. Am. Chem. Soc.*, 1997, **119**, 10956–10962.
- 33 C. S. Campos-Fernandez, B. L. Schottel, H. T. Chifotides, J. K. Bera, J. Bacsa, J. M. Koomen, D. H. Russell and K. R. Dunbar, *J. Am. Chem. Soc.*, 2005, **127**, 12909–12923.
- 34 B. Olenyuk, A. Fechtenkötter and P. J. Stang, *J. Chem. Soc., Dalton Trans.*, 1998, 1707–1728.
- 35 M. Ferrer, L. Rodriguez and O. Rossell, *J. Organomet. Chem.*, 2003, **681**, 158–166.
- 36 A. Sautter, D. G. Schmid, G. Jung and F. Würthner, *J. Am. Chem. Soc.*, 2001, **123**, 5424–5430.
- 37 M. Schweiger, S. R. Seidel, A. M. Arif and P. J. Stang, *Inorg. Chem.*, 2002, **41**, 2556–2559.
- 38 M. Schweiger, S. R. Seidel, A. M. Arif and P. J. Stang, *Angew. Chem., Int. Ed.*, 2001, **40**, 3467–3469.
- 39 M. Fujita, O. Sasaki, T. Mitsuhashi, T. Fujita, J. Yazaki, K. Yamaguchi and K. Ogura, *Chem. Commun.*, 1996, 1535–1536.
- 40 P. J. Stang, D. H. Cao, S. Saito and A. M. Arif, *J. Am. Chem. Soc.*, 1995, **117**, 6273–6283.
- 41 M. Fujita, S. Nagao, M. Iida, K. Ogata and K. Ogura, *J. Am. Chem. Soc.*, 1993, **115**, 1574–1576.
- 42 M. Fujita, J. Yazaki and K. Ogura, *Tetrahedron Lett.*, 1991, **32**, 5589–5592.
- 43 A. Sautter, D. G. Schmid, G. Jung and F. Würthner, *J. Am. Chem. Soc.*, 2001, **123**, 5424–5430.

- 44 S. J. Lee, J. S. Kim and W. Lin, *Inorg. Chem.*, 2004, **43**, 6579–6588.
- 45 D. K. Chand, M. Fujita, K. Biradha, S. Sakamoto and K. Yamaguchi, *Dalton Trans.*, 2003, 2750–2756.
- 46 M. Ferrer, M. Mounir, O. Rossell, E. Ruiz and M. A. Maestro, *Inorg. Chem.*, 2003, **42**, 5890–5899.
- 47 Z. Qin, M. C. Jennings and R. J. Puddephatt, *Inorg. Chem.*, 2003, **42**, 1956–1965.
- 48 P. Ballester, M. Capo, A. Costa, P. M. Deya, A. Frontera and R. Gomila, *Molecules*, 2004, **9**, 278–286.
- 49 Z. Qin, M. C. Jennings and R. J. Puddephatt, *Chem. Commun.*, 2001, 2676–2677.
- 50 T. J. Burchell, D. J. Eisler and R. J. Puddephatt, *Dalton Trans.*, 2005, 268–272.
- 51 P. Diaz, D. M. P. Mingos, R. Vilar, A. J. P. White and D. J. Williams, *Inorg. Chem.*, 2004, **43**, 7597–7604.
- 52 E. Doxiadi, R. Vilar, A. J. P. White and D. J. Williams, *Polyhedron*, 2003, **22**, 2991–2998.
- 53 D. Rais, D. M. P. Mingos, R. Vilar, A. J. P. White and D. J. Williams, *J. Organomet. Chem.*, 2002, **652**, 87–93.
- 54 D. Rais, J. Yau, M. P. Mingos, R. Vilar, A. J. P. White and D. J. Williams, *Angew. Chem., Int. Ed.*, 2001, **40**, 3464–3467.
- 55 S.-T. Cheng, E. Doxiadi, R. Vilar, A. J. P. White and D. J. Williams, *J. Chem. Soc., Dalton Trans.*, 2001, 2239–2244.
- 56 R. Vilar, D. M. P. Mingos, A. J. P. White and D. J. Williams, *Chem. Commun.*, 1999, 229–230.
- 57 R. Vilar, D. M. P. Mingos, A. J. P. White and D. J. Williams, *Angew. Chem., Int. Ed.*, 1998, **37**, 1258–1261.
- 58 P. Diaz, J. Benet-Buchholz, R. Vilar and A. J. P. White, *Inorg. Chem.*, 2006, **45**, 1617–1626.
- 59 J. J. Kane, R.-F. Liao, J. W. Lauher and F. W. Fowler, *J. Am. Chem. Soc.*, 1995, **117**, 12003–12004.
- 60 L. J. Barbour, G. W. Orr and J. L. Atwood, *Nature*, 1998, **393**, 671–673.
- 61 N. S. Goroff, S. M. Curtis, J. A. Webb, F. W. Fowler and J. W. Lauher, *Org. Lett.*, 2005, **7**, 1891–1893.
- 62 T. L. Nguyen, F. W. Fowler and J. W. Lauher, *J. Am. Chem. Soc.*, 2001, **123**, 11057–11064.
- 63 B.-C. Tzeng, Y.-C. Huang, B.-S. Chen, W.-M. Wu, S.-Y. Lee, G.-H. Lee and S.-M. Peng, *Inorg. Chem.*, 2007, **46**, 186–195.
- 64 The change in temperature could also favor the increase of the concentration of one of the species in equilibrium.
- 65 A concentration change should have no effect on the ratio of conformers since both exchanging partners become equally diluted. On the other hand, a change of concentration in the adequate range has a profound impact in the speciation of supramolecular self-assembled aggregates.
- 66 A. R. Sanger, *J. Chem. Soc., Dalton Trans.*, 1977, 1971–1976.
- 67 I. R. Butler, W. R. Cullen, T. J. Kim, S. J. Rettig and J. Trotter, *Organometallics*, 1985, **4**, 972–980.
- 68 G. M. Sheldrick, *SHELXTL Crystallographic System Ver. 5.10*, Bruker AXS, Inc., Madison, WI, 1998.
- 69 A. L. Spek, *Acta Crystallogr., Sect. A*, 1990, **A46**, C34.